Originally published in Bulletin of Earthquake Engineering (2007) with DOI: 10.1007/s10518-007-9050-5
The final publication is available at http://link.springer.com

# Non-Linear Seismic Behavior of Structures with Limited Hysteretic Energy Dissipation Capacity

PIERINO LESTUZZI[1,*], YOUSSEF BELMOUDEN[1] and MARTIN TRUEB[2]

[1]IS-Structural Engineering Institute, EPFL-Ecole Polytechnique Fédérale de Lausanne
[2]IBK-Structural Engineering Institute, ETHZ-Swiss Federal Institute of Technology Zurich
[*]Corresponding author:
EPFL ENAC IS IMAC, Bâtiment GC, Station 18, CH-1015 Lausanne, Switzerland.
Phone: +41 21 693 63 62; fax: +41 21 693 47 48; E-mail address: pierino.lestuzzi@epfl.ch

## Abstract

This paper investigates the non-linear seismic behavior of structures such as slender unreinforced masonry shear walls or precast post-tensioned reinforced concrete elements, which have little hysteretic energy dissipation capacity. Even if this type of seismic response may be associated with significant deformation capacity, it is usually not considered as an efficient mechanism to withstand strong earthquakes. The objective of the investigations is to propose values of strength reduction factors for seismic analysis of such structures. The first part of the study is focused on non-linear single-degree of freedom (SDOF) systems. A parametric study is performed by computing the displacement ductility demand of non-linear SDOF systems for a set of 164 recorded ground motions selected from the European Strong Motion Database. The parameters investigated are the natural frequency, the strength reduction factor, the post-yield stiffness ratio, the hysteretic energy dissipation capacity and the hysteretic behavior model (four different hysteretic models: bilinear self-centring, with limited or without energy dissipation capacity, modified Takeda and Elastoplastic). Results confirm that the natural frequency has little influence on the displacement ductility demand if it is below a frequency limit and vice versa. The frequency limit is found to be around 2 Hz for all hysteretic models. Moreover, they show that the other parameters, especially the hysteretic behavior model, have little influence on the displacement ductility demand. New relationships between the displacement ductility demand and the strength reduction factor for structures having little hysteretic energy dissipation capacity are proposed. These relationships are an improvement of the equal displacement rule for the considered hysteretic models. In the second part of the investigation, the parametric study is extended to multi-degree of freedom (MDOF) systems. The investigation shows that the results obtained for SDOF systems are also valid for MDOF systems. However, the SDOF system overestimates the displacement ductility demand in comparison to the corresponding MDOF system by approximately 15%.

KEYWORDS: displacement ductility demand, hysteretic energy, non-linear structural response, strength reduction factor, recorded earthquake, seismic analysis, rocking.

## 1. Introduction

This paper presents the main results gained during a research project performed at the Swiss Federal Institute of Technology in Lausanne (EPFL). The complete description of this work may be found in Trueb (2005). The research project addresses non-linear structural behavior in the context of seismic design and evaluation. Specifically, it aims to answer the following question: under what conditions can the strength reduction factor for structures with little hysteretic energy dissipation capacity be extended beyond the limit value of 1.5 proposed by the current construction codes? Note that the limit value of 1.5 in the construction codes does only consider overstrength and does therefore not include potential stable non-linear behavior.

### 1.1 Context

It is well established that structures do not remain elastic under extreme ground motion. Non-linear behavior therefore constitutes the key issue in seismic design and evaluation of structures. However, to avoid the use of more elaborate analysis, structural engineering methodologies are usually based on simplified static methods to determine seismic action. This particularly applies to design where such methodologies are still used, even with modern design concepts such as the capacity design method (Paulay and Priestley, 1992). In these simplified methods, compared to linear behavior, seismic action is reduced according to the deformation capacity and the energy dissipation capacity of the structure since it undergoes large inelastic deformations. More specifically, elastic response spectra and strength reduction factors are used. In other words, the strength reduction factor allows the use of linear

elastic analysis to estimate the maximum inelastic response. The majority of the building codes around the world are based on this design philosophy.

Intensive numerical investigations have already been performed to examine the relationships between strength reduction factors and the non-linear behavior of structures subjected to earthquake ground motions. This was done for both recorded and synthetic earthquakes (see Miranda (1994) for a review of significant investigations). The studies were generally focused on non-linear single-degree-of-freedom (SDOF) systems defined by different hysteretic models. However, the involved hysteretic models (elastoplastic, Clough, Takeda, etc.) were mostly related to seismic behavior with significant energy dissipation such as ductile reinforced concrete shear walls. Until recently, very few systematic investigations were carried out for structures with little hysteretic energy dissipation capacity such as slender unreinforced masonry shear walls that show very different seismic behavior (Christopoulos et al., 2002 and 2003). Figure 1 illustrates this fundamental difference with the hysteretic loops measured in dynamic tests on slender structural shear walls (Lestuzzi and Bachmann, 2007 and ElGawady et al., 2006). Even if both structural walls clearly behave in a non-linear manner, the hysteretic energy dissipation capacity is totally different. Ductile reinforced concrete shear walls (Figure 1, left) show significant hysteretic energy dissipation capacity. By contrast, unreinforced masonry shear walls (Figure 1, right) behave in a rocking mode associated with very little hysteretic energy dissipation. Other structures that show this type of behavior are precast post-tensioned reinforced concrete structures or concentrically braced steel structures with slender diagonal elements (Bruneau et al., 1998).

### 1.2 Equal displacement rule

Based on the results of the intensive numerical studies, empirical relationships were proposed. The equal displacement rule is the most popular one. As illustrated in Figure 2, the equal displacement rule states that inelastic peak displacements ($u_p$) are approximately equal to elastic peak displacements ($u_{el}$) whatever the selected yield strength ($F_y=F_{el}/R$ or yield displacement $u_y=u_{el}/R$) of the structure. Note that when assuming that the stiffness is independent of strength, the equal displacement rule leads to a strength reduction factor (R) equal to the global displacement ductility ($\mu_\Delta=u_p/u_y$). The equal displacement rule plays a significant role in current seismic design since it constitutes the basic assumption for the definition of the strength reduction factors (e. g. behavior factor q in EC8). The equal displacement rule was found to be generally correct and almost independent of the hysteretic model, for both real and synthetic earthquakes, and for structures with natural frequencies below a frequency limit (generally between 1.5 Hz and 2 Hz).

### 1.3 Methodology

Figure 3 illustrates the methodology used in this study. It consists of a systematic investigation of the non-linear response of SDOF systems subjected to a set of 164 earthquake recordings. These records are taken from the European Strong Motion Database (Ambraseys et al., 2002). The structural behavior is described by two hysteretic models developed for simulating limited hysteretic energy dissipation capacity. In addition, two recognised hysteretic models are included to serve as a reference.

Statistical analysis of the seismic response is performed for thirteen initial natural frequencies ($f_0$) representing the typical range of natural frequencies of buildings and for nine values of the strength reduction factor (R). The displacement ductility

demand is considered to be a representative indicator for the non-linear seismic behavior.

As some discrepancies between the characteristics in the seismic non-linear behavior of SDOF systems and multi-degree-of-freedom (MDOF) systems were already reported (Nassar and Krawinkler, 1991), the investigations are later extended to MDOF systems. The motivation behind this second part of the investigations is to test if the results obtained for SDOF systems hold true for MDOF systems representing buildings. For this purpose, several MDOF systems are subjected to the set of 164 recordings. Every story of the MDOF systems follows the same hysteretic behavior without hysteretic energy dissipation capacity. Statistical results are then compared with those of equivalent SDOF systems which were defined to have the same push-over curve as the corresponding MDOF systems.

**2. Ground motions**

Non-linear time history analysis may be carried out using both recorded earthquakes or artificially generated earthquakes. The reported investigations are focused on recorded earthquakes. Compared to recordings, synthetic earthquakes introduce additional uncertainties and bias that can strongly influence non-linear seismic behavior (Schwab and Lestuzzi, 2007).

164 registered ground acceleration time histories from the European Strong Motion Database (Ambraseys et al., 2002) are used. The selection of the recordings in the database is based on structural engineering considerations rather than seismological ones. As a consequence, earthquakes triggered in different geological conditions are

incorporated in the set. The main objective is to perform a statistical study of the non-linear response of structures undergoing any recorded earthquake.

In order to consider earthquakes that may produce significant non-linearities in the structural behavior, only recordings with a magnitude larger than 5 were considered. Figure 4 shows the magnitude-epicentral distance relationship of the set of 164 selected recordings. Their main characteristics are listed in the table in the appendix. The magnitudes range from 5.0 to 7.6, the epicentral distances range from 2 to 195 km and the peak ground accelerations (PGA) range from 0.61 to 7.85 $m/s^2$.

This data base was used in another research project in the field of seismic non-linear behavior in which criteria to choose suitable earthquake recordings for non-linear dynamic analyses of ductile structures were developed. As a result, predictions of the seismic impact on this type of structures could be improved (Lestuzzi et al., 2004).

**3. Investigations with SDOF systems**

According to the methodology illustrated in Figure 3, the following parameters are examined in the first part of the study with SDOF systems: the initial natural frequency, the strength reduction factor and the hysteretic energy dissipation capacity using four hysteretic models.

### 3.1 Definition and hysteretic models

The non-linear SDOF system is defined by the following parameters:

- the initial natural frequency $f_0$
- the strength reduction factor R
- the hysteretic model according to which the structure behaves in the non-linear range

Thirteen initial natural frequencies covering the range of frequencies of usual buildings are evaluated. The natural frequencies range from $f_0 = 0.25$ Hz to 4.0 Hz in steps of 0.25 Hz. Nine different values of strength reduction factors (R = 1.2, 1.4, 1.6, 1.8, 2.0, 2.5, 3.0, 3.5 and 4.0) are examined. The following hysteretic models are used to compute the non-linear responses: a bilinear self-centring model (S-model), a bilinear self-centring model with limited hysteretic energy dissipation capacity (Flag-model), an elastoplastic-model (EP-model) and the modified Takeda-model. The force-displacement relationships defining the four hysteretic models that are considered in the investigations are plotted in Figure 5 and described below:

1) **Bilinear self-centring model (S-model):** The bilinear self-centring hysteretic model is the simplest model to represent elements with little or no hysteretic energy dissipation capacity. It is called self-centring because it unloads such that there are no residual displacements when the external load is reduced to zero. Because of its shape, this model is called “S-model”. The post-yield stiffness is defined as being a fraction of the initial stiffness.

   Slender masonry shear walls show this sort of behavior when the failure mode is “rocking” and the other modes i.e. “sliding”, “shear failure” and “toe crushing” may be excluded (Figure 1, right). The elastic part of the force-displacement

relationships represents the usual flexural deformation of the masonry shear wall. Once the tensile strength is reached, large flexural cracks occur at the base of the cantilever shear wall. As the displacements increase, the shear wall behaves like a rigid body rotating about the compressed toe. When forces reverse, the flexural cracks close and the shear wall behaves like an uncracked one (this corresponds to the elastic branch of the force-displacement curve). The equilibrium is only ensured by external contact forces to the wall and its own weight. If the wall element is restrained by the concrete floor and the slabs of the ceiling this creates a certain amount of additional strength that can be interpreted as hardening in the plastic deformation.

The force-displacement relationship of the bilinear self-centring model is specified through three parameters: the initial stiffness, the yield displacement and the post-yield stiffness, expressed as a portion of the initial stiffness.

2) **Bilinear self-centring model with energy dissipation (Flag-model):** In order to refine the bilinear self-centring hysteretic model such that it represents the measured behavior more closely, a small amount of hysteretic energy dissipation capacity is implemented. The key concept is the introduction of a different unloading stiffness after the element has undergone plastic deformation. However, the self-centring aspect of the model is still preserved. It is assumed that the transition from elastic to plastic behavior will always occur at the same specified yield displacement. The amount of energy dissipation is controlled by adjusting the unloading stiffness (higher unloading stiffness produces more hysteretic energy dissipation). Because of its shape, this model is called “Flag-model”.

Comparing the hysteretic model from Figure 5 to the experimental curve shown in Figure 1 on the right-hand side one can observe that the model simulates the

correct behavior quite accurately. The main simplification from the experiment to the model is the assumption that the model is self-centring and the curve hence passes through the origin.

The force-displacement relationship of the Flag-model is specified through four parameters: the initial stiffness, the yield displacement, the post-yield stiffness and the unloading stiffness. The later two stiffnesses are expressed as a portion of the initial stiffness.

3)**Elastoplastic model (EP-model):** The elastoplastic model is sometimes also called bilinear model. Even if it is mainly intended for elastoplastic materials, such as steel, this model is extensively used for all types of materials due to its simplicity. It is included in this study because it is one of the standard models often taken as a reference in numerical simulations. The objective is to compare the hysteretic models with little hysteretic energy dissipation capacity, which are the main subject of this study, to the elastoplastic model that shows a large amount of energy dissipation.

The force-displacement relationship of the EP-model is specified using only three parameters: the initial stiffness, the yield displacement and the post-yield stiffness expressed as a portion of the initial stiffness.

4)**Modified Takeda-model:** The modified Takeda-model provides a much better simulation of the features of materials such as reinforced concrete than the EP-model. Specifically, the modified Takeda-model includes realistic conditions for the reloading curves and takes into account the degradation of the stiffness due to increasing damage, which is an important feature of reinforced concrete subjected to seismic loading (Saatcioglu, 1991). However, the modified Takeda-model does not account for strength degradation. The Takeda-model was initially proposed in an original version by Takeda et al. (1970). The modified

Takeda-model was developed independently by Otani (1974) and Litton (1975). It was later adapted by many researchers. The version used here is the one of Allahabadi and Powell (1988). The force-displacement relationship of the modified Takeda-model is specified through five parameters: the initial stiffness, the yield displacement, the post-yield stiffness, a parameter relating the stiffness degradation ($\alpha$) and a parameter ($\beta$) specifying the target for the reloading curve. In this study, the modified Takeda-model is used as a reference. Therefore, standard values of the parameters ($\alpha$=0.4 and $\beta$=0.0) are used in all analyses.

### 3.2 Results with SDOF systems

Relative displacements are used to represent the dynamic non-linear response. According to the value of the strength reduction factor, yield displacements are primarily determined through linear elastic analysis for each recording. By varying the initial fundamental frequency, the strength reduction factor and the hysteretic model, a single ground motion leads to 468 (13x9x4=468) different dynamic non-linear responses. Because the computations are repeated for each recording, 164 values are used to determine the average and standard deviation for each couple of strength reduction factor and initial fundamental frequency.

The results for the displacement ductility demand are presented first, in terms of mean values and in terms of variability. Later section relates the impact of the post-yield stiffness on the non-linear behavior of the SDOF systems. Finally, two simplified R-$\mu_\Delta$-T relationships for structures having limited hysteretic energy dissipation capacity are proposed.

### 3.2.1 Mean values of displacement ductility demand

The displacement ductility demand ($\mu_\Delta$) is defined as the ratio of the peak non-linear displacement to the yield displacement. The displacement ductility demand varies strongly between different considered ground motions but mean values obtained from a large number of ground motions show clear tendencies. Typical results are illustrated in Figures 6 and 7. The plotted results correspond to a post-yield stiffness equal to 10% of the initial stiffness for all the hysteretic models. For Flag-model, the unloading stiffness is equal to 20% of the initial stiffness.

The plots in Figures 6 and 7 show very similar tendencies for all hysteretic models. As expected, larger displacement ductility demands are related to hysteretic models with smaller hysteretic energy dissipation capacity (Figure 6). However, the differences are not pronounced. Moreover, the general shape of the curves is conserved. The displacement ductility demand stays more or less constant for frequencies below 2 Hz and afterwards increases with increasing frequency.

### 3.2.2 Variability of displacement ductility demand

Besides mean values, variability is the main statistical characteristic of the displacement ductility demand. Typical results are illustrated in Figure 8 for one value of the strength reduction factor (R = 3). In order to characterize the variability, the mean values (solid line) are plotted together with mean values plus one standard deviation and mean values minus one standard deviation (dotted lines) as a function of the initial frequency of the SDOF systems. Similar to Figures 6 and 7, the plotted results correspond to a post-yield stiffness equal to 10% of the initial stiffness. Based on the plots of Figure 8, the comparison between the S-model and the modified Takeda-model shows that even if variability is significantly larger for the S-model, there are similarities in both hysteretic models. Variability stays

approximately constant for frequencies below 2 Hz and significantly increases afterwards.

It should be noted that singularities in displacement ductility demand appear for the very low frequencies between 0.25 and 0.5 Hz (see Figures 6 to 8). Not much importance is attached to this observation because this is probably an undesired effect produced by the noise in the ground acceleration measurements. The seismometers are often not adequately equipped to measure very low frequencies and so the recorded ground acceleration time history is corrupted, which leads to the found result. A fact that supports this conclusion is that this effect appears regardless of the hysteretic model used and for all ground motions and strength reduction factors.

### 3.2.3 Post-yield stiffness

To avoid falsifying the parametric study of the post-yield stiffness ratio (hardening coefficient), the S-model is used instead of the Flag-model. For the Flag-model, the hysteretic energy dissipation capacity is directly influenced by the variation of the post-yield stiffness ratio. The results of the study are shown in Figure 9 for a selected value of the initial frequency ($f_0$=2 Hz) and a selected value of the strength reduction factor (R=2). The influence of the post-yield stiffness ratio is insignificant. Some hysteretic curves are plotted in Figure 9 (left) to highlight the influence of hardening. As expected, the displacement ductility demand decreases with increasing post-yield stiffness ratio. However, in the range of reasonable hardening coefficients for structures having limited hysteretic energy dissipation capacity, the influence of hardening on the displacement ductility demand is minimal (Figure 9, right). The mean values of displacement ductility demand (solid line) are plotted together with mean values plus one standard deviation and mean values minus one standard deviation (dotted lines) as a function of the hardening

coefficient in Figure 9 (right). The displacement ductility demand is found to be linear. Note that, of course the displacement ductility demand approaches the value of the considered strength reduction factor as the hardening coefficient increases to 100%, which would represent elastic behavior.

### 3.3 A simplified formulation for R-$\mu_\Delta$-T relationships

The main objective of the research project is to propose strength reduction factor-displacement ductility demand relationships for structures with limited capacity of hysteretic energy dissipation. However, similar to the equal displacement rule, the formulation should remain as simple as possible. In brief, for structures with limited capacity of hysteretic energy dissipation, the study is focused on the improvement of the equal displacement rule for the frequency range below 2 Hz, particularly for strength reduction factors between 2 and 3. Figure 6 shows that the equal displacement rule ($\mu_\Delta = R$) leads to underestimating the results for both the S-model and the Flag-model and for all frequencies above 0.5 Hz. By contrast, the usual competing empirical rule of equal energy ($\mu_\Delta = R^2/2 + 1/2$) leads to largely overestimated results for strength reduction factors above R=2 (for instance, $\mu_\Delta = 5$ for R=3). Consequently convenient relationships should lie between these two common empirical rules. As a boundary condition, the relationships should lead to $\mu_\Delta = 1$ for R=1. Based on the results of the parametric study, a simplified formulation for R-$\mu_\Delta$-T relationships is proposed as follows:

$$\mu_\Delta = \frac{3}{2}R - \frac{1}{2} \tag{1}$$

$$\mu_\Delta = \frac{4}{3}R - \frac{1}{3} \tag{2}$$

The proposed R-$\mu_\Delta$ relationships are printed in Figure 10 and plotted together with the obtained results of Figure 6. Thus, for structures without any hysteretic energy

dissipation capacity, Equation (1) is used. For structures with a limited hysteretic energy dissipation capacity, Equation (2) is recommended. The relationships (1) and (2) are set to be valid in terms of mean values for the frequency range below 2 Hz and for strength reduction factors between 2 and 3. The relationships should be adjusted if they are to be used for higher strength reduction factors. One suggested modification consists of removing the constant member in the proposed relationships.

The proposed relationships are slightly different for the S-model and for the Flag-model. As expected, Equation (2) is closer to the equal displacement rule than Equation (1). Note that for R=2, Equation (1) and the empirical equal energy rule lead to identical results ($\mu_\Delta$=2.5).

Figure 7 confirms that the equal displacement rule is valid for ductile structures whose seismic behavior may be modelled by the modified Takeda-model. Figure 7 shows that this is exactly true for frequencies below 2 Hz and for strength reduction factors up to R=3. By contrast, the empirical rule is not very accurate for the EP-model.

**3.4 Findings for SDOF systems**

The parametric study on SDOF systems resulted in the following important findings. The most astonishing revelation is, that the chosen hysteretic model has limited influence on the displacement ductility demand. In other words, hysteretic models with little hysteretic energy dissipation capacity do not lead to excessive displacement ductility demand. The hysteretic energy dissipation capacity is seen to have only little effect on the displacement ductility demand. Note that since

different yield displacements are used for the definition of the non-linear SDOF system, the results for the displacement demand do not correspond to those for the displacement ductility demand.

The displacement ductility demand is influenced by the ground acceleration time history, the initial natural frequency of the SDOF system and the strength reduction factor. Generally, the investigated parameters: the hardening coefficient and the slope of the unloading branch of the Flag-model show little to no influence on the displacement ductility demand irrespective of the values considered for the initial natural frequency or the strength reduction factor.

The equal displacement rule is approximately satisfied for frequencies below 2 Hz but has a tendency to slightly underestimate the displacement ductility demand for the S-model and for the Flag-model. However the empirical rule is accurate for the modified Takeda-model. Thus, more accurate displacement ductility demand - strength reduction factor relationships for the S-model and for the Flag-model are formulated.

**4. Investigations with MDOF systems**

In order to verify the validity of the above conclusions obtained for SDOF systems for multistorey structural wall buildings, a second investigation is performed with MDOF systems. Non-linear responses are computed using the same database of 164 recordings. The same type of non-linear constitutive law according to the S-model is used for every storey of the MDOF system. Since it was found that in the case of SDOF systems the hysteretic energy dissipation has little influence on the

displacement ductility demand, the investigations were not extended to a non-linear constitutive law such as the Flag-model.

### 4.1 Definition of MDOF systems

Figure 11 shows an example of the structures which were used in this part of the study. The model represents a building with four stories. The mass of the building is modelled as a concentrated mass (M) at each story level and it is kept the same for every story. The slabs are considered infinitely rigid in their in-plane direction and no rotational degrees of freedom are introduced. Each story has one horizontal lateral displacement degree of freedom. All the stories are modelled with the same hysteretic model, namely the S-model. This hypothesis is based on the assumption that the slabs are infinitely rigid and therefore every wall element between the slabs can undergo a rocking behavior with no coupling effect. All other failure mechanisms, such as sliding or shear, are excluded. Moreover the use of only one simple constitutive law for all stories enables the comparison between SDOF and MDOF systems.

In contrast to the SDOF system, the MDOF system is defined by the story stiffness. In accordance with a Rayleigh-type damping model, a value of 5% damping ratio is assumed for the modes 1 and 2. The selection of the first and the second mode of vibration ensures a damping ratio greater than or equal to 5% for all modes. An accurate comparison between the MDOF system and its corresponding SDOF system is then possible since the influence of higher modes is limited by their larger damping ratios.

The determination of the displacement ductility demand is carried out for a 2 story, a 4 story and a 6 storey building model. The parametric study is performed for four values of the initial story stiffness (K=100N/m, 500N/m, 1000N/m and 2000N/m) and for four values of the strength reduction factor (R=1.5, 2, 3 and 4).

The mean values of the displacement ductility demand (for 164 ground motion records) are computed for all considered cases of stiffness summarized in Table 1. The mass of every story was chosen to have a total mass of unity. The resulting fundamental frequency for all MDOF systems investigated is given in Table 1. The hardening ratio of the constitutive law is set to 10%.

**4.2 Equivalent SDOF system**

To ensure a relevant comparison of the results between MDOF and SDOF systems, equivalent SDOF systems are defined for each MDOF system. An equivalent SDOF system follows the same hysteretic model as the stories of the corresponding MDOF system (S-model). Thus both systems have the same initial fundamental frequency. However, the post-yield stiffness for the equivalent SDOF system should be calibrated to reproduce the same global behavior as the corresponding MDOF system. The equivalence is determined on the basis of push-over curves and leads to a modification (multiplication) of the hardening coefficient for equivalent SDOF systems (1.2 times for 2 DOF, 0.8 times for 4 DOF and 0.7 times for 6 DOF systems).

**4.3 Yield displacement**

Before computing the non-linear response, the yield displacement should be defined. In the considered MDOF systems, plastification is governed by the relative

displacements between stories. So, plastification will first occur for the story with the largest relative displacements. Consequently, the yield displacement is defined as being the peak relative displacement between any two stories during the linear elastic response divided by the strength reduction factor. This is the case for the relative displacement between the first story and the ground level unless a mode other than the first mode is dominant.

### 4.4 Displacement ductility demand

The computation of the displacement ductility demand with MDOF systems is not as straightforward as with SDOF systems. It is important to distinguish between local and global ductility. The R-$\mu_\Delta$-T relationships are expressed for global displacement ductility demands. For example, the equal displacement rule is formulated for the global displacement ductility demand of a structure. Therefore, the comparison of the displacement ductility demand between SDOF and MDOF systems needs to be done on the basis of the global displacement ductility demand. The local ductility demand can also be of interest if it is compared to the ductility capacity of an element. This is beyond the scope of this study. The global displacement ductility demand is defined as the peak non-linear displacement at the top of the building divided by the top displacement at the stage when the first element reaches its yield relative displacement. The global yield displacement is the peak linear elastic displacement of the top of the building divided by the corresponding strength reduction factor.

### 4.5 Results with MDOF systems

The displacement ductility demand is chosen as a representative value for the non-linear behavior. In function of the value of the strength reduction factor, the yield

displacement is computed through linear elastic analysis. In virtue of the discussion above, the global ductility is used to compute the displacement ductility demand. The results are plotted in Figure 12 as a function of the fundamental frequencies of the examined structures.

The plots of Figure 12 show that the equivalent SDOF system (right) generally overestimates the displacement ductility demand when compared to the corresponding MDOF system (left). The difference lies between 10% and 15%. In the adopted methodology, some equivalent SDOF systems have a similar initial natural frequency (see Table 1) but a quite different post-yield stiffness ratio. This explains the abrupt drops in the force-displacement curves of the equivalent SDOF systems (Figure 12, right).

**4.6 Findings with MDOF systems**

The main finding of this second part of the study is that the displacement ductility demand of a MDOF system and its corresponding equivalent SDOF system is roughly the same. However, the equivalent SDOF system has a tendency to overestimate the displacement ductility demand by about 15%. This means that all the results obtained by the parametric study on SDOF systems are also relevant for MDOF systems.

The computations show that the plastic hinge formation is primarily concentrated at the base of the MDOF structures. Consequently, the local ductility demand is higher in the lower stories and decreases rapidly towards the top of the structure where the behavior can be considered as elastic. This confirms that the local ductility demand is considerably higher than the global displacement ductility demand.

The consequence for practical engineering is that a SDOF model for a building is admissible when analyzing the displacement ductility demand. The SDOF system overestimates the displacement ductility demand and thereby it is a conservative model. However, it is important to define the corresponding SDOF system with caution. Both SDOF and MDOF systems are roughly equivalent, if their "push over" curves are similar.

## 5. Summary and conclusions

In this paper, the seismic response of structures that show a non-linear behavior with little hysteretic energy dissipation capacity such as slender unreinforced masonry shear walls or precast post-tensioned reinforced concrete elements is investigated. The displacement ductility demand is computed for a set of 164 registered ground motions from the European Strong Motion Database. Statistical analyses are performed to characterize seismic performance. The obtained results reveal that hysteretic models with limited hysteretic energy dissipation capacity definitely do not lead to excessive displacement ductility demand. This is an important result that contradicts the widely held perception of hysteretic models without hysteretic energy dissipation capacity. It is often assumed that this kind of structural behavior is not an efficient mechanism to withstand strong earthquakes, even if it may be associated with significant deformation capacity. In the light of the presented results it is found that hysteretic energy dissipation capacity is not the unique characteristic of a good seismic behavior. The non-linear behavior due to the transition between initial stiffness and post-yield stiffness is the main favourable aspect that affects seismic behavior.

Note that since different yield displacements are considered for the definition of the non-linear systems, the results obtained for the displacement ductility demand may not be extended to those for the displacement demand.

The results obtained by the parametric study performed on non-linear SDOF systems show that the displacement ductility demand is influenced by the ground acceleration time history, the initial natural frequency and the strength reduction factor. On the contrary, parameters such as the hardening coefficient and a small hysteretic energy dissipation capacity have little to no influence on the displacement ductility demand. This is found to be independent of the considered initial natural frequency or the strength reduction factor.

Based on the results, new strength reduction factor - displacement ductility demand relationships are proposed for hysteretic models with little to no hysteretic energy dissipation capacity (S-model and Flag-model). For these models, in the frequency range below 2 Hz, the equal displacement rule provides only a rough approximation, as it always underestimates the displacement ductility demand. The proposed relationships represent improved empirical rules for structures with a limited capacity of hysteretic energy dissipation.
Compared to non-linear SDOF systems, similar seismic behavior is also seen in MDOF systems. However, the SDOF system has a tendency to overestimate the displacement ductility demand of the corresponding MDOF system by about 15%.

The following design recommendations should be retained:

• Strength reduction factors larger than 1.5 may be used for structures having limited hysteretic energy dissipation capacity.

• For seismic behavior related to limited hysteretic energy dissipation capacity, the SDOF system is on the "safe side" when analyzing the ductility demand compared to the MDOF system.

The upper-limit value of 1.5, currently beeing recommended by the design codes for strength reduction factors of structures with limited hysteretic energy dissipation capacity considering only their overstrength is definitely too conservative. As long as the structural elements have a large displacement capacity, strength reduction factors up to 3 can be adopted. Note that additional attention should be paid to the fact that no other structural failure mechanism can take place and that strength degradation may be excluded. For frequencies below 2 Hz a prediction of the displacement ductility demand may be obtained by using the proposed R-$\mu_\Delta$-T relationships. This conclusion is important for many cases. One example are slender unreinforced masonry elements subjected exclusively to the "rocking" failure mode. The proposed relationships are also applicable for structures such as those that use precast post-tensioned reinforced concrete elements.

In applying the results of this study certain caution is recommended. The main source of concern is the important variability of the displacement ductility demand in function of the considered ground motion. Before using the findings pointed out herein in structural design and analysis, a study with ground motions that were adjusted to the design spectrum of the considered site should be conducted, in order to minimize the variability of the results. In other words, the obtained results are only valid qualitatively not quantitatively. It is also strongly recommended that the numerical results be validated by practical experiments.

## 6. References

Allahabadi R. and Powell G. H. (1988) Drain-2DX User Guide. Report No. UCB/EERC-88/06. College of Engineering, University of California, Berkeley.

Ambraseys, N., Smit, P., Sigbjornsson, R., Suhadolc, P. and Margaris, B. (2002), Internet-Site for European Strong-Motion Data, European Commission, Research-Directorate General, Environment and Climate Programme.

Bruneau M., Chia-Ming U. and Whittaker A. (1998) Ductile Design of Steel Structures. McGraw-Hill, New York.

Christopoulos C., Filiatrault A. and Folz B. (2002) Seismic response of self-centring hysteretic SDOF systems. Earthquake Engineering and Structural Dynamics, Vol. 31, pp.1131-1150.

Christopoulos C., Pampanin S. and Priestley M.J.N. (2003) Performance-Based Seismic Response of Frame Structures Including Residual Deformations. Part I: Single-Degree-Of-Freedom Systems. Journal of Earthquake Engineering, Vol. 7, No. 1, pp. 97-118.

ElGawady M. A., Lestuzzi P. and Badoux M. (2006) Aseismic retrofitting of unreinforced masonry walls using FRP. Composites Part B. Vol 37, pp. 148-162.

Eurocode 8 (2004). Design of Structures for Earthquake Resistance, Part 1: General Rules, Seimic Actions and Rules for Buildings, EN 1998-1; 2004; European Committee for Standardization (CEN), Brussel.

Lestuzzi P., Schwab P., Koller M. and Lacave C. (2004) How to Choose Earthquake Recordings for Non-linear Seismic Analysis of Structures. *Proceedings of 13th World Conference on Earthquake Engineering*, Vancouver, British Columbia, Canada.

Lestuzzi P. and Bachmann H. (2007) Displacement ductility and energy assessment from shaking table tests on RC structural walls. Engineering Structures. Vol 29/8, pp. 1708-1721.

Litton R. W. (1975) A contribution to the analysis of concrete structures under cyclic loading. Ph.D. Thesis, Civil Engineering Dept., University of California, Berkeley.

Miranda E. and Bertero V. (1994) Evaluation of Strength Reduction Factors for Earthquake-Resistant Design. Earthquake Spectra. Vol 10, No. 2, pp. 357-379.

Nassar A.A. and Krawinkler H. (1991) Seismic Demands for SDOF and MDOF Systems. Research Report No. 95, The John A. Blume Earthquake Engineering Center, Department of Civil Engineering, Stanford University, Stanford, California.

Otani A. (1974) Inelastic analysis of R/C frame structures. J. Struct. Div., ASCE 100 ST7, 1433-1449.

Paulay T. and Priestley M. J. N. (1992) Seismic Design of Reinforced Concrete and Masonry Buildings. John Wiley & Sons, New York.

Saatcioglu M. (1991) Modeling hysteretic force deformation relationships for R/C elements. *Earthquake-Resistant Concrete Structures: Inelastic Response and Design. Special publication SP-127 of the American Concrete Institute (ACI)*. Detroit, Michigan.

Schwab P. and Lestuzzi P. (2007) Assessment of the seismic non-linear behavior of ductile wall structures due to synthetic earthquakes. Bulletin of Earthquake Engineering. Vol 5/1, pp. 67-84.

Takeda T., Sozen M. A. and Nielsen N. N. (1970) Reinforced concrete response to simulated earthquakes. *Journal of the Structural Division. Proceedings of the American Society of Civil Engineers (ASCE)*. Vol. 96, No. ST12.

Trueb M. (2005) Seismic behaviour of non-linear elements with little energy dissipation. Master thesis, Ecole Polytechnique Fédérale de Lausanne (EPFL), Switzerland.

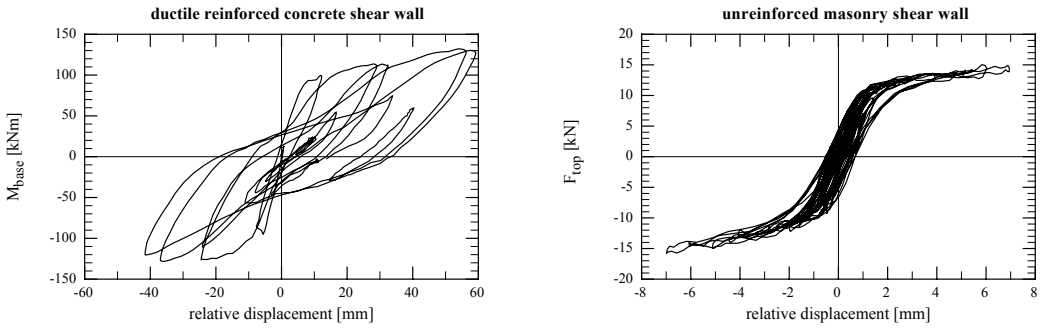


Figure 1: Measured hysteresis loops in dynamic tests on slender structural shear walls. Ductile reinforced concrete shear walls (Lestuzzi and Bachmann, 2007, left) and slender unreinforced masonry shear walls (ElGawady et al., 2006, right).

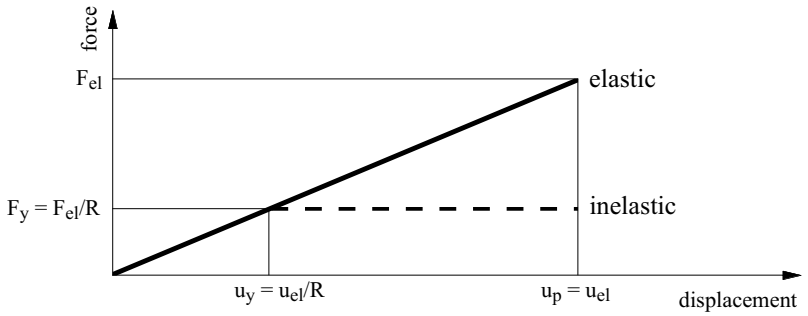


Figure 2: Elastic and inelastic force-displacement relationships relating the empirical equal displacement rule.

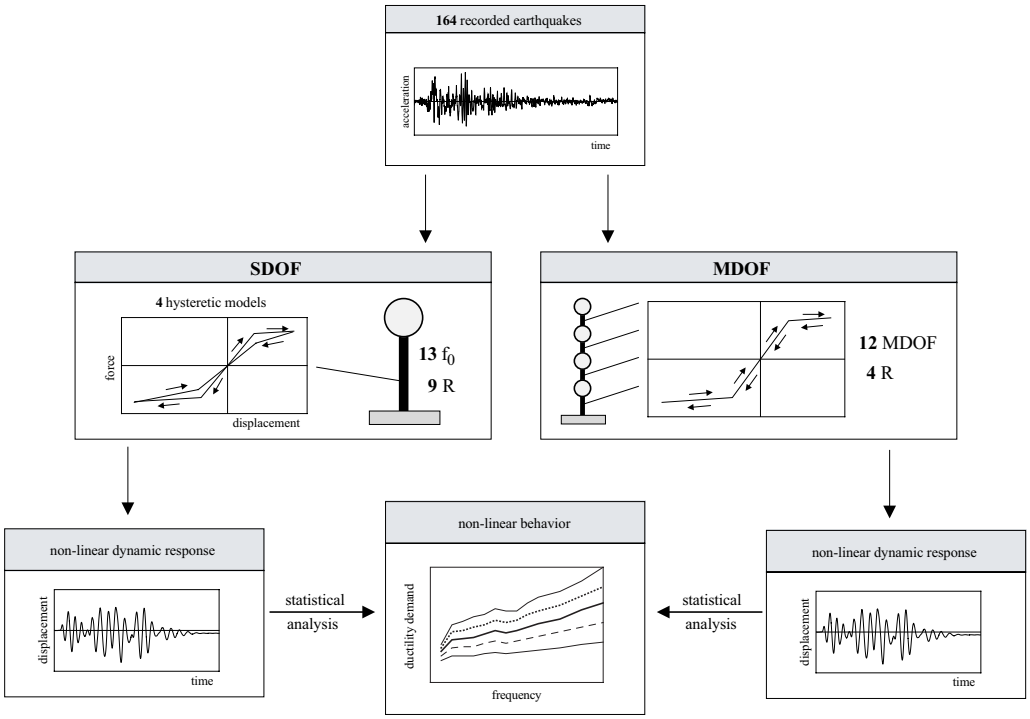


Figure 3: Schematic description of the followed methodology.

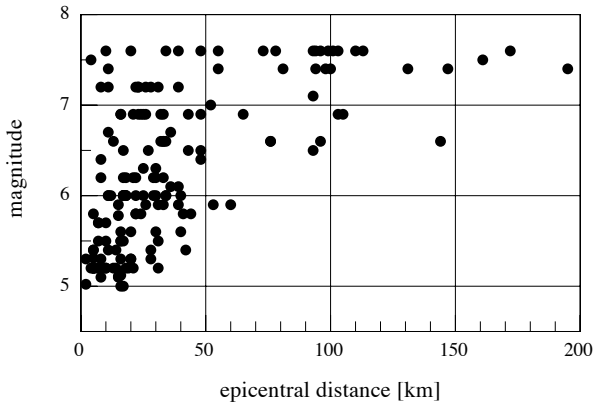


Figure 4: Magnitude-epicentral distance relationship of the 164 recordings of the used database.

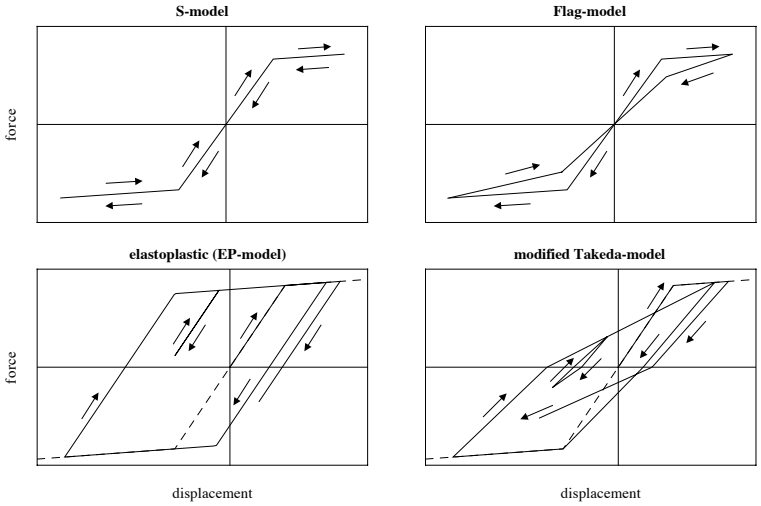


Figure 5: The four hysteretic models that are used in the investigations with non-linear SDOF systems.

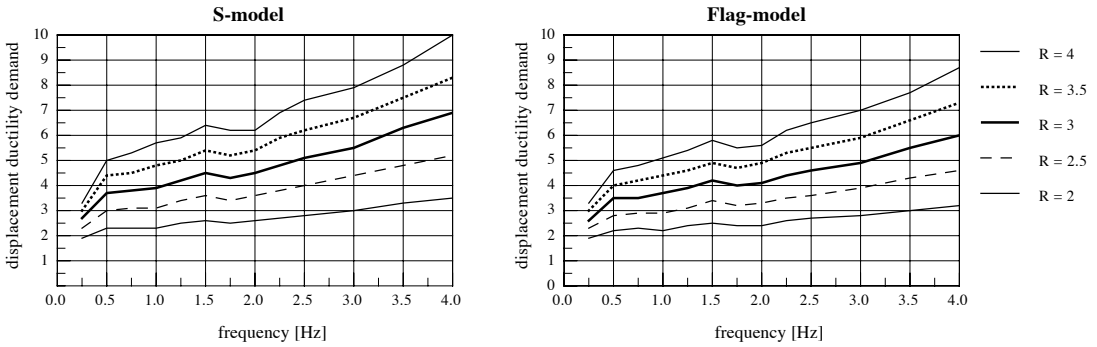


Figure 6: Mean values of the displacement ductility demand as a function of the initial frequency of the SDOF system for different strength reduction factors (R). S-model (left) and Flag-model (right).

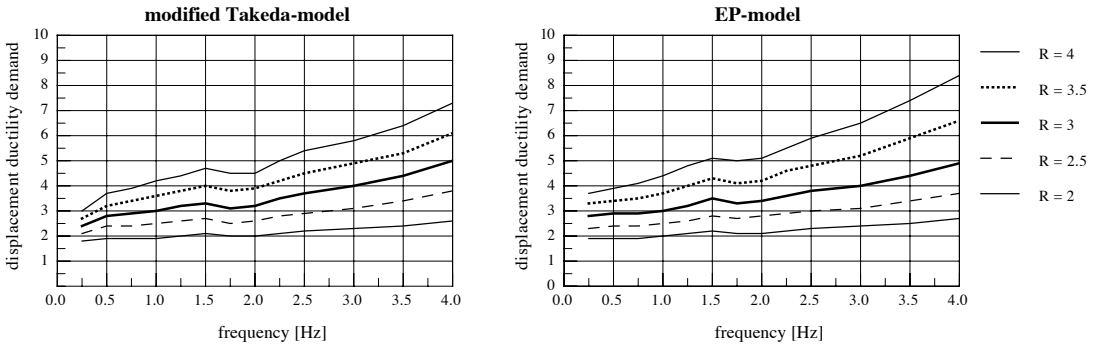


Figure 7: Mean values of the displacement ductility demand as a function of the initial frequency of the SDOF system for different strength reduction factors (R). Modified Takeda-model (left) and Elastoplastic-model (right).

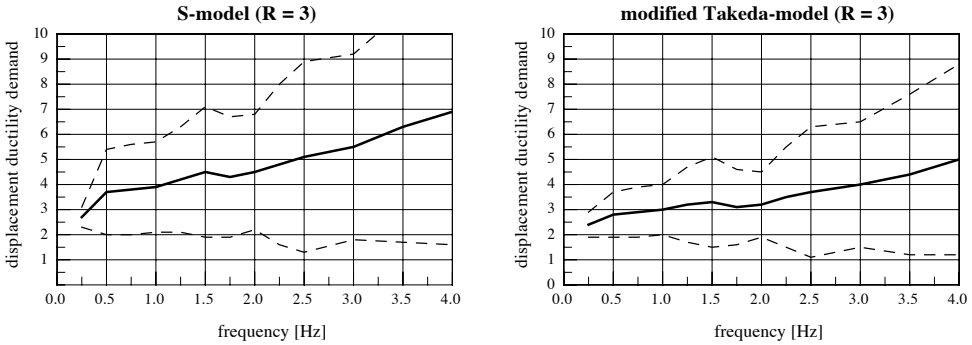


Figure 8: Variability of the displacement ductility demand. Mean values (solid line), mean values plus one standard deviation and mean values minus one standard deviation (dotted lines) as a function of the initial frequency of the SDOF system for one value of the strength reduction factor (R=3). S-model (left) and modified Takeda-model (right).

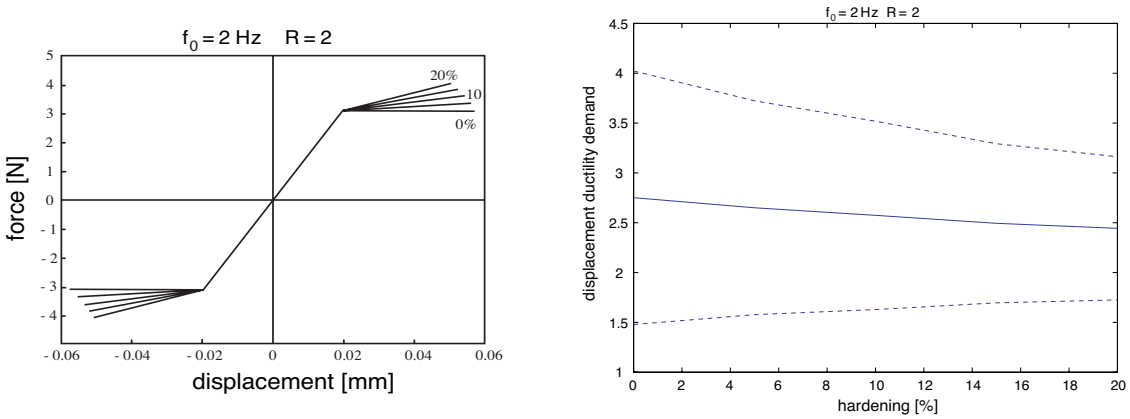


Figure 9: The impact of hardening is very limited. Force-displacement relationships for different values of hardening (left). The displacement ductility demand is decreasing for an increasing hardening coefficient. It follows a linear relationship as a function of hardening coefficient (right).

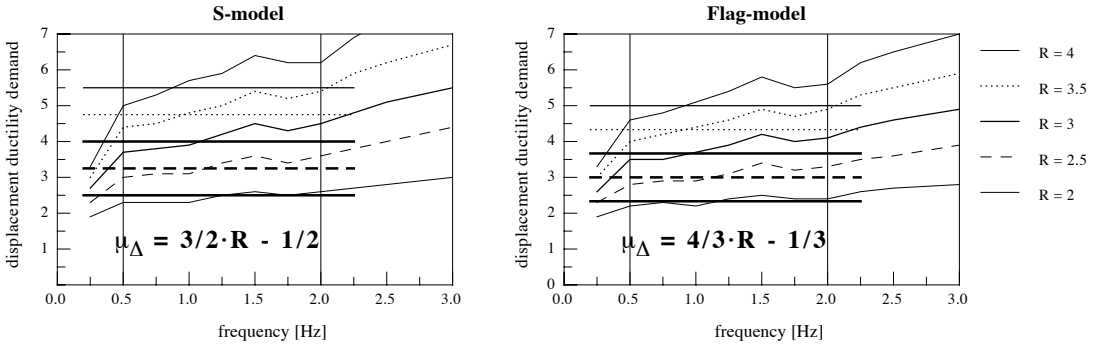


Figure 10: Proposed R-$\mu_\Delta$ relationships in comparison with the obtained results of Figure 6. The relationships are set to be valid for the frequency range below 2 Hz and for strength reduction factors between 2 and 3.

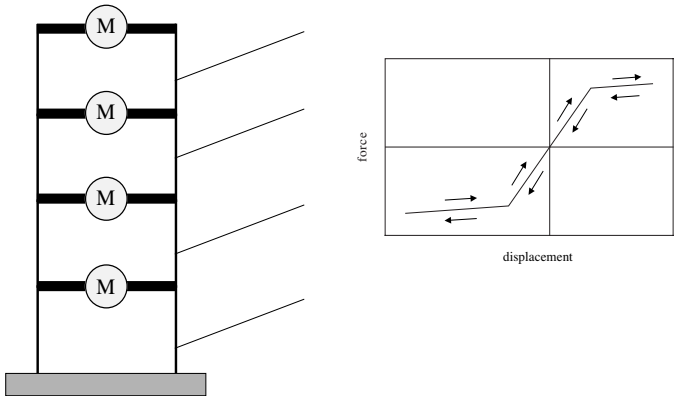


Figure 11: Sketch for a four story structure used in the MDOF systems investigations. The mass (M) is the same for every stories. The slabs are considered to be infinitely rigid. The same S-model is used for the hysteretic behavior of every story (right).

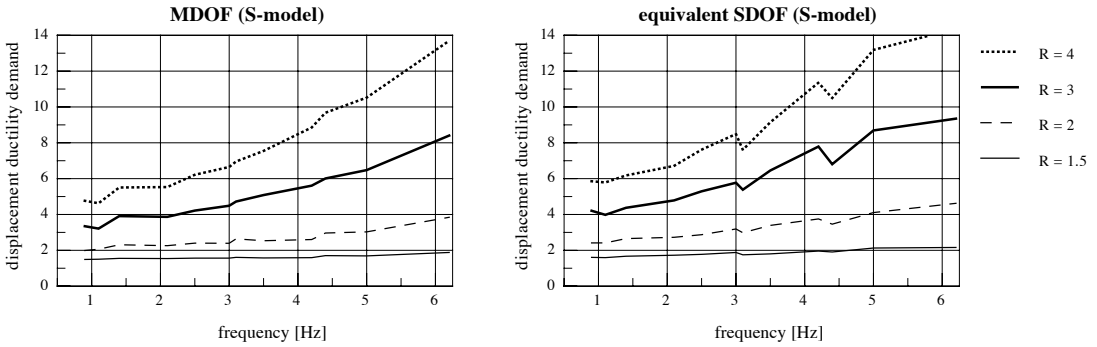


Figure 12: Mean values of the displacement ductility demands as a function of the first natural frequency for different strength reduction factors (R). MDOF systems (left) and related equivalent SDOF systems (right).

Table 1: First natural frequencies of the examined MDOF systems.

| Initial stiffness [N/m] | Frequency [Hz] | | |
|---|---|---|---|
| | 2 DOF | 4 DOF | 6 DOF |
| 100 | 1.4 | 1.1 | 0.9 |
| 500 | 3.1 | 2.5 | 2.1 |
| 1000 | 4.4 | 3.5 | 3.0 |
| 2000 | 6.2 | 5.0 | 4.2 |

## Appendix

Table: Main characteristics of the 164 recordings composing the used data base.

| Earthquake | Date | Station | Magnitude | Component | PGA [m/s2] | Δ [km] |
|---|---|---|---|---|---|---|
| Azores | 23.11.1973 | San Mateus | 5.31Ms | x | 2.688 | 5 |
| Friuli (aftershock) | 07.05.1976 | Tolmezzo-Diga Ambiesta | 5.2Mw | x | 1.247 | 31 |
| Denizli | 19.08.1976 | Denizli-Bayindirlik ve Iskan Mudurlugu | 5.11Ms | x | 3.386 | 15 |
| Friuli (aftershock) | 11.09.1976 | Breginj-Fabrika IGLI | 5.3Mw | y | 1.701 | 16 |
| Friuli (aftershock) | 11.09.1976 | Forgaria-Cornio | 5.3Mw | y | 1.075 | 20 |
| Friuli (aftershock) | 11.09.1976 | Kobarid-Osn.Skola | 5.3Mw | y | 0.96 | 28 |
| Friuli (aftershock) | 11.09.1976 | San Rocco | 5.3Mw | y | 0.684 | 20 |
| Friuli (aftershock) | 11.09.1976 | Tarcento | 5.3Mw | x | 1.931 | 8 |
| Friuli (aftershock) | 11.09.1976 | Buia | 5.5Mw | x | 2.26 | 10 |
| Friuli (aftershock) | 11.09.1976 | Forgaria-Cornio | 5.5Mw | y | 2.273 | 16 |
| Friuli (aftershock) | 11.09.1976 | Kobarid-Osn.Skola | 5.5Mw | y | 0.916 | 31 |
| Friuli (aftershock) | 11.09.1976 | San Rocco | 5.5Mw | x | 0.898 | 16 |
| Friuli (aftershock) | 16.09.1977 | Forgaria-Cornio | 5.4Mw | x | 2.365 | 5 |
| Friuli (aftershock) | 16.09.1977 | San Rocco | 5.4Mw | x | 0.997 | 5 |
| Friuli (aftershock) | 16.09.1977 | Somplago Centrale-Uscita Galleria | 5.4Mw | x | 1.869 | 11 |
| Friuli (aftershock) | 16.09.1977 | Tolmezzo-Diga Ambiesta | 5.4Mw | y | 0.91 | 14 |
| Izmir | 16.12.1977 | Izmir-Meteoroloji Istasyonu | 5.02Ms | x | 2.051 | 2 |
| Calabria | 11.03.1978 | Ferruzzano | 5.2Mw | y | 0.762 | 10 |
| Volvi | 04.07.1978 | Thessaloniki-City Hotel | 5.12Ms | x | 1.125 | 16 |
| Almiros (aftershock) | 11.08.1980 | Almiros Volos-Town Hall | 5.2Mw | y | 0.705 | 14 |
| El Asnam (aftershock) | 08.11.1980 | Beni Rashid | 5.2Mw | x | 0.946 | 18 |
| Campano Lucano (aftershock) | 16.01.1981 | Cairano 1 | 5.2Mw | y | 1.521 | 5 |
| Campano Lucano (aftershock) | 16.01.1981 | Cairano 2 | 5.2Mw | y | 1.66 | 5 |
| Campano Lucano (aftershock) | 16.01.1981 | Cairano 3 | 5.2Mw | y | 1.499 | 6 |
| Campano Lucano (aftershock) | 16.01.1981 | Cairano 4 | 5.2Mw | y | 0.705 | 7 |
| Campano Lucano (aftershock) | 16.01.1981 | Contrada Fiumicella-Teora | 5.2Mw | x | 1.081 | 4 |
| Campano Lucano (aftershock) | 16.01.1981 | Conza-Base | 5.2Mw | y | 0.963 | 5 |
| Campano Lucano (aftershock) | 16.01.1981 | Conza-Vetta | 5.2Mw | y | 0.865 | 5 |
| Campano Lucano (aftershock) | 16.01.1981 | Lioni-Macello | 5.2Mw | x | 0.629 | 8 |
| Campano Lucano (aftershock) | 16.01.1981 | Procisa Nuova | 5.2Mw | y | 1.057 | 8 |
| Preveza | 10.03.1981 | Lefkada-OTE Building | 5.4Mw | y | 0.971 | 42 |
| Preveza | 10.03.1981 | Preveza-OTE Building | 5.4Mw | x | 1.402 | 28 |
| Kefallinia (aftershock) | 17.01.1983 | Argostoli-OTE Building | 5.2Mw | x | 0.767 | 10 |
| Ierissos | 26.08.1983 | Ierissos-Police Station | 5.1Mw | y | 1.79 | 8 |
| Ierissos | 26.08.1983 | Ouranoupolis-Seismograph Station | 5.1Mw | y | 1.273 | 15 |
| Lazio Abruzzo (aftershock) | 11.05.1984 | Atina-Pretura Terrazza | 5.5Mw | x | 1.411 | 17 |
| Lazio Abruzzo (aftershock) | 11.05.1984 | Villetta-Barrea | 5.5Mw | y | 2.111 | 7 |
| Near SE coast of Zakynthos island | 04.10.1984 | Zakynthos-OTE Building | 5Mw | y | 0.774 | 17 |
| Near SE coast of Zakynthos island | 04.10.1984 | Pelekanada-Town Hall | 5Mw | y | 1.766 | 16 |
| Near coast of Preveza | 31.08.1985 | Lefkada-Hospital | 5.2Mw | x | 0.727 | 21 |
| Near coast of Preveza | 31.08.1985 | Preveza-OTE Building | 5.2Mw | x | 0.856 | 13 |
| Drama | 09.11.1985 | Drama-Prefecture | 5.2Mw | y | 0.834 | 19 |
| Skydra-Edessa | 18.02.1986 | Edessa-Prefecture | 5.3Mw | x | 0.852 | 2 |
| Ionian | 04.11.1973 | Lefkada-OTE Building | 5.78Ms | x | 5.146 | 15 |
| Friuli (aftershock) | 15.09.1976 | Breginj-Fabrika IGLI | 6Mw | y | 4.956 | 18 |
| Friuli (aftershock) | 15.09.1976 | Buia | 6Mw | x | 1.069 | 11 |
| Friuli (aftershock) | 15.09.1976 | Codroipo | 6Mw | x | 0.701 | 40 |
| Friuli (aftershock) | 15.09.1976 | Forgaria-Cornio | 6Mw | x | 2.586 | 17 |
| Friuli (aftershock) | 15.09.1976 | Kobarid-Osn.Skola | 6Mw | y | 1.201 | 30 |
| Friuli (aftershock) | 15.09.1976 | Robic | 6Mw | x | 0.998 | 25 |
| Friuli (aftershock) | 15.09.1976 | San Rocco | 6Mw | y | 1.202 | 17 |
| Friuli (aftershock) | 15.09.1976 | Breginj-Fabrika IGLI | 6Mw | y | 4.136 | 22 |
| Friuli (aftershock) | 15.09.1976 | Buia | 6Mw | y | 0.884 | 12 |
| Friuli (aftershock) | 15.09.1976 | Forgaria-Cornio | 6Mw | x | 3.395 | 17 |
| Friuli (aftershock) | 15.09.1976 | Kobarid-Osn.Skola | 6Mw | x | 1.392 | 34 |
| Friuli (aftershock) | 15.09.1976 | Robic | 6Mw | x | 0.868 | 29 |

| Earthquake | Date | Station | Magnitude | Component | PGA [m/s2] | Δ [km] |
|---|---|---|---|---|---|---|
| Friuli (aftershock) | 15.09.1976 | San Rocco | 6Mw | y | 2.319 | 17 |
| Friuli (aftershock) | 15.09.1976 | Tarcento | 6Mw | x | 1.339 | 11 |
| Basso Tirreno | 15.04.1978 | Milazzo | 6Mw | y | 0.728 | 34 |
| Basso Tirreno | 15.04.1978 | Naso | 6Mw | x | 1.493 | 18 |
| Basso Tirreno | 15.04.1978 | Patti-Cabina Prima | 6Mw | y | 1.585 | 18 |
| Montenegro (aftershock) | 15.04.1979 | Bar-Skupstina Opstine | 5.8Mw | y | 0.813 | 41 |
| Montenegro (aftershock) | 15.04.1979 | Hercegnovi Novi-O.S.D. Pavicic School | 5.8Mw | x | 0.908 | 22 |
| Montenegro (aftershock) | 15.04.1979 | Petrovac-Hotel Oliva | 5.8Mw | x | 0.976 | 24 |
| Valnerina | 19.09.1979 | Arquata del Tronto | 5.8Mw | y | 0.87 | 22 |
| Valnerina | 19.09.1979 | Cascia | 5.8Mw | y | 2.012 | 5 |
| Valnerina | 19.09.1979 | Nocera Umbra | 5.8Mw | x | 0.815 | 44 |
| NE of Banja Luka | 13.08.1981 | Banja Luka-Borik 2 | 5.7Mw | y | 2.555 | 7 |
| NE of Banja Luka | 13.08.1981 | Banja Luka-Borik 9 | 5.7Mw | x | 3.551 | 7 |
| NE of Banja Luka | 13.08.1981 | Banja Luka-Seismograph Station | 5.7Mw | y | 0.74 | 10 |
| Heraklio | 19.03.1983 | Heraklio-Prefecture | 5.6Mw | y | 1.782 | 40 |
| Umbria | 29.04.1984 | Gubbio | 5.6Mw | y | 0.655 | 16 |
| Umbria | 29.04.1984 | Nocera Umbra | 5.6Mw | x | 2.045 | 30 |
| Umbria | 29.04.1984 | Pietralunga | 5.6Mw | y | 1.846 | 20 |
| Lazio Abruzzo | 07.05.1984 | Atina | 5.9Mw | y | 1.08 | 15 |
| Lazio Abruzzo | 07.05.1984 | Garigliano-Centrale Nucleare 1 | 5.9Mw | y | 0.609 | 53 |
| Lazio Abruzzo | 07.05.1984 | Ortucchio | 5.9Mw | y | 0.852 | 26 |
| Lazio Abruzzo | 07.05.1984 | Ponte Corvo | 5.9Mw | y | 0.671 | 31 |
| Lazio Abruzzo | 07.05.1984 | San Agapito | 5.9Mw | x | 0.69 | 33 |
| Lazio Abruzzo | 07.05.1984 | Scafa | 5.9Mw | x | 1.292 | 60 |
| Lazio Abruzzo | 07.05.1984 | Taranta Peligna | 5.9Mw | y | 0.751 | 39 |
| Friuli | 06.05.1976 | Codroipo | 6.5Mw | y | 0.86 | 48 |
| Friuli | 06.05.1976 | Conegliano-Veneto | 6.5Mw | y | 0.712 | 93 |
| Friuli | 06.05.1976 | Tolmezzo-Diga Ambiesta | 6.5Mw | x | 3.499 | 27 |
| Volvi | 20.06.1978 | Thessaloniki-City Hotel | 6.2Mw | y | 1.43 | 29 |
| Montenegro (aftershock) | 24.05.1979 | Bar-Skupstina Opstine | 6.2Mw | y | 2.652 | 33 |
| Montenegro (aftershock) | 24.05.1979 | Budva-PTT | 6.2Mw | y | 2.624 | 8 |
| Montenegro (aftershock) | 24.05.1979 | Hercegnovi Novi-O.S.D. Pavicic School | 6.2Mw | y | 0.754 | 30 |
| Montenegro (aftershock) | 24.05.1979 | Kotor-Zovod za Biologiju Mora | 6.2Mw | y | 1.487 | 22 |
| Montenegro (aftershock) | 24.05.1979 | Petrovac-Hotel Rivijera | 6.2Mw | y | 2.703 | 17 |
| Montenegro (aftershock) | 24.05.1979 | Tivat-Aerodrom | 6.2Mw | x | 1.627 | 21 |
| Alkion | 25.02.1981 | Korinthos-OTE Building | 6.3Mw | y | 1.176 | 25 |
| Kefallinia (aftershock) | 23.03.1983 | Argostoli-OTE Building | 6.2Mw | y | 2.303 | 18 |
| Griva | 21.12.1990 | Edessa-Prefecture | 6.1Mw | x | 0.987 | 36 |
| Bitola | 01.09.1994 | Florina-Cultural Center | 6.1Mw | y | 0.795 | 39 |
| Kozani | 13.05.1995 | Kozani-Prefecture | 6.5Mw | x | 2.039 | 17 |
| Aigion | 15.06.1995 | Patra-San Dimitrios Church | 6.5Mw | y | 0.911 | 43 |
| Dinar | 01.10.1995 | Dinar-Meteoroloji Mudurlugu | 6.4Mw | y | 3.131 | 8 |
| Kalamata | 13.10.1997 | Koroni-Town Hall (Library) | 6.4Mw | x | 1.184 | 48 |
| Adana | 27.06.1998 | Ceyhan-Tarim Ilce Mudurlugu | 6.3Mw | y | 2.644 | 30 |
| Gazli | 17.05.1976 | Karakyr Point | 6.7Mw | y | 7.065 | 11 |
| Caldiran | 24.11.1976 | Maku | 7Mw | x | 0.956 | 52 |
| Montenegro | 15.04.1979 | Bar-Skupstina Opstine | 6.9Mw | x | 3.68 | 16 |
| Montenegro | 15.04.1979 | Dubrovnik-Pomorska Skola | 6.9Mw | y | 0.735 | 105 |
| Montenegro | 15.04.1979 | Hercegnovi Novi-O.S.D. Pavicic School | 6.9Mw | y | 2.509 | 65 |
| Montenegro | 15.04.1979 | Petrovac-Hotel Oliva | 6.9Mw | x | 4.453 | 25 |
| Montenegro | 15.04.1979 | Ulcinj-Hotel Albatros | 6.9Mw | y | 2.198 | 21 |
| Montenegro | 15.04.1979 | Ulcinj-Hotel Olimpic | 6.9Mw | x | 2.88 | 24 |
| Campano Lucano | 23.11.1980 | Bagnoli-Irpino | 6.9Mw | y | 1.776 | 23 |
| Campano Lucano | 23.11.1980 | Bisaccia | 6.9Mw | x | 0.903 | 26 |
| Campano Lucano | 23.11.1980 | Brienza | 6.9Mw | x | 2.224 | 43 |
| Campano Lucano | 23.11.1980 | Calitri | 6.9Mw | y | 1.725 | 16 |
| Campano Lucano | 23.11.1980 | Mercato San Severino | 6.9Mw | y | 1.362 | 48 |
| Campano Lucano | 23.11.1980 | Rionero in Vulture | 6.9Mw | y | 0.975 | 33 |
| Campano Lucano | 23.11.1980 | Sturno | 6.9Mw | y | 3.166 | 32 |
| Alkion | 24.02.1981 | Korinthos-OTE Building | 6.6Mw | y | 3.036 | 33 |

| Earthquake | Date | Station | Magnitude | Component | PGA [m/s2] | Δ [km] |
|---|---|---|---|---|---|---|
| Alkion | 24.02.1981 | Xilokastro-OTE Building | 6.6Mw | x | 2.838 | 34 |
| Kefallinia island | 17.01.1983 | Lefkada-Hospital | 6.9Mw | x | 0.641 | 103 |
| Off coast of Magion Oros peninsula | 06.08.1983 | Ouranoupolis-Seismograph Station | 6.6Mw | x | 1.066 | 76 |
| Panisler | 30.10.1983 | Horasan-Meteoroloji Mudurlugu | 6.6Mw | y | 1.575 | 33 |
| Spitak | 07.12.1988 | Gukasian | 6.7Mw | y | 1.796 | 36 |
| Erzincan | 13.03.1992 | Erzincan-Meteorologij Mudurlugu | 6.6Mw | y | 5.028 | 13 |
| | | Refahiye-Kaymakamlik Binasi | | x | 0.691 | 76 |
| Strofades | 18.11.1997 | Koroni-Town Hall (Library) | 6.6Mw | y | 0.907 | 144 |
| Strofades | 18.11.1997 | Kyparrisia-Agriculture Bank | 6.6Mw | y | 0.723 | 96 |
| Strofades | 18.11.1997 | Zakynthos-OTE Building | 6.6Mw | x | 1.289 | 32 |
| Bucharest | 04.03.1977 | Bucharest-Building Research Institute | 7.5Mw | x | 1.976 | 161 |
| Bucharest | 04.03.1977 | Vrancioaia | 7.5Mw | x | 1.905 | 4 |
| Tabas | 16.09.1978 | Bajestan | 7.4Mw | y | 1.858 | 147 |
| Tabas | 16.09.1978 | Boshroyeh | 7.4Mw | x | 1.003 | 55 |
| Tabas | 16.09.1978 | Dayhook | 7.4Mw | y | 3.779 | 11 |
| Tabas | 16.09.1978 | Ferdoos | 7.4Mw | y | 1.002 | 100 |
| Manjil | 20.06.1990 | Abhar | 7.4Mw | y | 2.047 | 98 |
| Manjil | 20.06.1990 | Gachsar | 7.4Mw | y | 1.033 | 195 |
| Manjil | 20.06.1990 | Qazvin | 7.4Mw | x | 1.804 | 94 |
| Manjil | 20.06.1990 | Rudsar | 7.4Mw | x | 0.951 | 81 |
| Manjil | 20.06.1990 | Tonekabun | 7.4Mw | x | 1.341 | 131 |
| Gulf of Akaba | 22.11.1995 | Eilat | 7.1Mw | y | 0.894 | 93 |
| Izmit | 17.08.1999 | Ambarli-Termik Santrali | 7.6Mw | x | 2.58 | 113 |
| Izmit | 17.08.1999 | Botas-Gas Terminal | 7.6Mw | y | 0.974 | 172 |
| Izmit | 17.08.1999 | Cekmece-Kucuk | 7.6Mw | x | 1.698 | 110 |
| Izmit | 17.08.1999 | Duzce-Meteoroloji Mudurlugu | 7.6Mw | y | 3.542 | 99 |
| Izmit | 17.08.1999 | Fatih-Tomb | 7.6Mw | x | 1.756 | 94 |
| Izmit | 17.08.1999 | Gebze-Arcelik | 7.6Mw | x | 2.047 | 55 |
| Izmit | 17.08.1999 | Gebze-Tubitak Marmara Arastirma Merkezi | 7.6Mw | x | 2.334 | 48 |
| Izmit | 17.08.1999 | Goynuk-Devlet Hastanesi | 7.6Mw | x | 1.347 | 73 |
| Izmit | 17.08.1999 | Heybeliada-Senatoryum | 7.6Mw | y | 1.04 | 78 |
| Izmit | 17.08.1999 | Istanbul-Atakoy | 7.6Mw | y | 1.611 | 101 |
| Izmit | 17.08.1999 | Istanbul-Mecidiyekoy | 7.6Mw | y | 0.618 | 93 |
| Izmit | 17.08.1999 | Istanbul-Zeytinburnu | 7.6Mw | y | 1.12 | 96 |
| Izmit | 17.08.1999 | Izmit-Meteoroloji Istasyonu | 7.6Mw | y | 2.192 | 10 |
| Izmit | 17.08.1999 | Iznik-Karayollari Sefligi Muracaati | 7.6Mw | y | 1.266 | 39 |
| Izmit | 17.08.1999 | Sakarya-Bayindirlik ve Iskan Mudurlugu | 7.6Mw | y | 3.542 | 34 |
| Izmit | 17.08.1999 | Yarimca-Petkim | 7.6Mw | x | 2.903 | 20 |
| Izmit | 17.08.1999 | Yesilkoy-Havaalani | 7.6Mw | x | 0.871 | 103 |
| Duzce 1 | 12.11.1999 | Bolu-Bayindirlik ve Iskan Mudurlugu | 7.2Mw | y | 7.85 | 39 |
| Duzce 1 | 12.11.1999 | Duzce-Meteoroloji Mudurlugu | 7.2Mw | y | 5.036 | 8 |
| Duzce 1 | 12.11.1999 | IRIGM Station No. 487 | 7.2Mw | y | 2.902 | 22 |
| Duzce 1 | 12.11.1999 | IRIGM Station No. 498 | 7.2Mw | y | 3.824 | 23 |
| Duzce 1 | 12.11.1999 | LDEO Station No. C1058 BV | 7.2Mw | x | 1.091 | 11 |
| Duzce 1 | 12.11.1999 | LDEO Station No. C1059 FP | 7.2Mw | y | 1.539 | 23 |
| Duzce 1 | 12.11.1999 | LDEO Station No. C1061 | 7.2Mw | x | 1.24 | 31 |
| Duzce 1 | 12.11.1999 | LDEO Station No. C1062 FI | 7.2Mw | x | 2.495 | 28 |
| Duzce 1 | 12.11.1999 | LDEO Station No. D0531 WF | 7.2Mw | y | 1.545 | 26 |